Spring 5-2020

Hemodynamic Effects on Aortic Development Due to Outflow Tract Banding

Humza Ismail
Washington University in St. Louis

Washington University in St. Louis

McKelvey School of Engineering

Department of Department Name

Thesis Examination Committee:

Jessica Wagenseil, Chair

Spencer Lake

Amit Pathak

Hemodynamic Effects on Aortic Development Due to Outflow Tract Banding

By

Humza Naveed Ismail

A thesis presented to the McKelvey School of Engineering of Washington University in St. Louis in partial fulfillment of the requirements for the degree of Master of Science

April 2020

St. Louis, Missouri

Dedication

To my parents, Naveed Ismail and Aliya Rajput, and the rest of my family for the unwavering support.

Acknowledgements

I would also like to thank my lab mates: Austin, Jie, Amy, Diana, and Gaby as well as Dr. Wagenseil for her guidance and support.

Table of Contents

List of Tables

Table of Figures

Abstract

Hemodynamic Effects on Aortic Development Due to Outflow Tract Banding

By

Humza Naveed Ismail

Master of Science in Mechanical Engineering

Washington University in St. Louis, 2020

Research Advisor: Professor Jessica Wagenseil

Hemodynamic forces drive remodeling of the early cardiac system in embryonic development. Perturbations of normal cardiac blood flow can cause the formation of defects and malformations within the cardiac system. Specifically, changes in hemodynamics can cause the formation of different congenital heart defects. The formation of heart defects has been studied; however, vasculature specific defects caused by changes in blood flow patterns in the early cardiac system have not been studied to the same degree. In this thesis, the effects of hemodynamic changes on arterial development were studied. Outflow tract banding (OTB) was used to cause a local increase in peak blood flow velocity in the outflow tract (OFT) of the early chick embryonic heart and resultant changes in the downstream dorsal aorta (DA) were studied. OTB was performed at 3 days of incubation, the suture was removed 24 hours later, and the embryo was studied at different time points up to 18 days of incubation. Hemodynamic measurements were taken at the OFT and the DA before and after OTB to see how changes in blood flow patterns in the early embryonic cardiac system affect development of the DA and its extracellular matrix (ECM) proteins. Elastin and collagen were of specific interest. Doppler ultrasound was used to show that OTB led to an increase in blood velocity in the OFT after banding and a decrease in

velocity in the DA after 3 days of incubation (immediately after suture removal). No difference in DA velocity was seen at 10 days of incubation (6 days after suture removal). Two-photon imaging was used to show that changes in blood flow velocity due to OTB caused no discernable difference in aortic elastin or collagen organization through 11 days of incubation. It is likely that longer incubation periods (beyond 11 days) are needed in future work to investigate changes in the DA ECM amount and organization due to OTB.

Chapter 1: Background

When studying development and disease, it is useful to use animal models as an analog to studying the behavior of humans. In particular, animal models serve as a way to study the effect that developmental and genetic defects can play in the formation of key physiological and anatomical features of the body. One of the diseases that can be studied with the use of animal models is congenital heart disease. Congenital heart disease (CHD) is the most common and lethal structural disease that is seen in newborn babies and only 20% of the cases at birth can be linked to a genetic defect (Midgett, Thornburg, & Rugonyi, 2017). The incidence of CHD at birth has been reported to be in 4/1000 to 50/1000 births with potentially 6/1000 to 19/1000 of those cases being moderate to severe (Hoffman & Kaplan, 2002).

Murine models have been of particular interest when it comes to investigating genetic defects linked to CHD. Transgenic and targeted genetic murine models are of particular use because one can directly reproduce gene expression seen in disease. However, genetic models have the disadvantage not being able to control the effect of null alleles or overexpression of a gene. Additional murine models of CHD include surgical interventions to change hemodynamic conditions and chemical applications to change cellular amounts or phenotypes Table 1.1 is a summary of the advantages and disadvantages of different mouse CHD models.

Model	Advantages	Limitations
Surgical		
Aortic banding	Model of human pressure overload	High mortality; technically demanding; relevance to other conditions?
Coronary ligation	Directly applicable to human disease	
Cryoinjury	Technically simple	Relevance to human disease?
Toxic		
Ethanol	Non-invasive; technically simple; reproducible	High mortality; non-cardiac effects; not generally applicable?
Doxorubicin		
Homocysteine		
Genetic		
Transgenic	Directly reproduces gene expression changes seen in disease	Non-specific effects of overexpression
Targeted		Developmental effects of null allele
Inducible null/transgenic	Control of time course of induction/deletion	Control of level of transgene often impossible

Table 1.1 Summary of the different types of mouse models for CHD (Breckenridge, 2010).

For developmental biology, the chick embryo is of particular use due to the ease of access to the embryo, whether it be in ovo or ex ovo, and ease of manipulation. Also, chick cardiovascular development is something that is relatively conserved relative to human and mouse embryonic development. For early development models, comparing animal models to humans becomes easier due to the similarity in shape of early embryos, something that is seen in mammals and non-mammals. This principle is known as von Baer's first law which states that the general features of a large group of animals appear earlier in development than the features that are shared by a smaller group of animals, a phenomenon that can be observed in Figure 1.1, which compares embryo shape of different species (Gilbert, 2000).

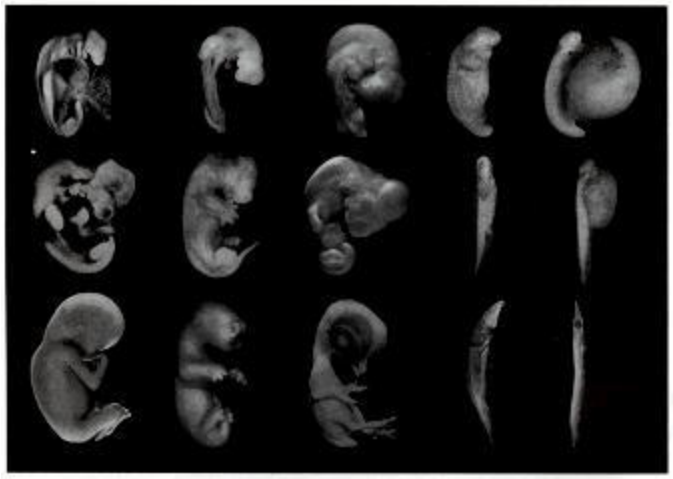

Figure 1.1. A comparison on the similarity in shape across species of the early embryo. Known as von Baer's first law, this attribute allows for the use of animal models when studying human development (Gilbert 2000).

Mice and chicks also share the same gestational period of 21 days, making comparisons between the two models easier. A comparison of the timeline of different cardiovascular events in humans, mice, and chicks is shown in Table 1.2 (Espinosa, Taber, & Wagenseil, 2018). Unlike murine models however, the ease of access to the embryo in ovo makes early embryonic interventions in the chick more favorable than interventions done in mice.

Event	Mouse Embryonic Age	Chick HH Stages (Embryonic Age)	Human Streeter Stages (Embryonic Age)
First Heart Beat	8d	9 (1.29d)	X (22d)
Blood Flow Begins	8.5d	10 (1.46d)	X (22d)
SMC Gene Expression in Aorta	11.5d	18 (2.79d)	
Elastin Expression in Aorta	16d	29 (6.5d)	XVII (35d)
Collagen Expression in Aorta	16d	32 (7.5d)	
Gestational Period	21d	(21d)	(274d)

Table 1.2 Timeline of Cardiovascular development in humans, mice and chick embryology (Espinosa 2018).

Changes in hemodynamics of the early embryonic heart are a useful tool and indicator of possible defects in cardiac development. For example, it has been shown that hemodynamic changes were seen before defects in chick embryonic heart development after neural crest ablation where the neural crest fold over somites 1 and 3 was ablated (Stewart, Kirby, & Sulik, 1986). A slight increase in dorsal aortic blood velocity was seen before a consistent onset of truncus arteriosus was seen. It has also been shown that conoctuncal banding in chicks embryos leads to a thickening to the myocardium, mild to severe ventricular dilation with some sort of ventricular septal defect occurring in every banded embryo such as the right atrioventricular valve becoming bicuspid in nature (Sedmera, Pexieder, Rychterova, Hu, & Clark, 1999). Hemodynamics play such an important role in early embryonic cardiac development, that the degree of altered hemodynamic load was correlated with the number of defects seen within a group. It was shown that degree of band tightness in chick embryos where the outflow tract (OFT) had been restricted (outflow tract banding, OTB) was related to the number of defects seen within an experimental group (Midgett et al., 2017).

Regional mechanical loading has been shown to have an effect on the passive properties of cardiac tissue during cardiogenesis. In a study where HH Stage 21 (3.5 day old) embryos either underwent Left arterial ligation (LAL) or conotruncal banding (CTB), embryos were found to change passive myocardial stiffness parameters to compensate for the alteration of flow and strain (Tobita, Schroder, Tinney, Garrison, & Keller, 2002). Hamburger-Hamilton stages are set developmental stages that define chick embryo development; they are based off development of features instead of incubation time (Hamburger & Hamilton, 1992). LAL was also used as a model for left heart hypoplasia, where right ventricles of ligated embryos were slow to remodel to increase pressure loads, leading to a high mortality rate in ligated embryos and showing the

right ventricles inability to act as a systemic pump (Sedmera et al., 1999). It was further shown that LAL shifted the embryonic heart to having a preferential circumferential strain pattern in the right ventricle from the left ventricle, indicating that wall stress distributions is critical in normal and altered morphogenesis (Tobita & Keller, 2000).

Changes in hemodynamics are also thought to have an effect on development at the cellular level. Endothelial cells are sensitive to changes in wall shear stress (WSS) that accompany changes in flow characteristics associated with altering normal blood flow through the early embryonic heart. Cultured vascular endothelial cells have been shown to respond to shear stress as low in magnitude as 0.2 dyn cm^{-2} and that there is a strong correlation between low shear stress and atherosclerotic lesions (Olesen, Claphamt, & Davies, 1988). Furthermore, it was shown in zebrafish that wall shear stress in the early embryonic heart ranged from 2.5 dyn cm^{-2} to 76 dyn cm^{-2} and that disrupting flow leads to the third chamber of the heart not forming and the absence of cardiac looping, causing a majority of embryos to dies before day 7 (Hove et al., 2003). Hemodynamic changes in early embryonic development influence endothelial cells in their arrangement of cytoskeletal structure and in gene expression (Ma et al., 2017). Increases in shear stress have been shown to increase endothelial cell elongation and stiffness at least temporarily and areas of disturbed or oscillatory flow are more prone to atherosclerosis prone (Li, Haga, & Chien, 2005).

Chick embryos have been used as a model of CHD through surgical interventions that alter hemodynamic loads, as discussed above. The effects that altered hemodynamics have on the development of the heart have been characterized, but the effects on dorsal aortic development has not been characterized. Additionally, while cellular changes in response to altered hemodynamics have been investigated in the heart and to some extent arteries, it is unknown

how hemodynamic changes affect the extracellular matrix components, including elastin and collagen, that are critical for determining the passive mechanical properties of the large, elastic arteries. It was the goal of this thesis to explore how altered hemodynamics affected the development of elastin in the dorsal aorta, with a specific focus on elastin and collagen.

Chapter 2: Chick Development

Stages of development are tracked through Hamburger Hamilton (HH) stages. In 1951, Viktor Hamilton and Howard L. Hamilton published their study of the staging of chick embryonic development. Their goal was to create a standard of normal development staging that was independent of time, and rather used the immergence of developmental features as landmarks to describe the developmental process of the chicken embryo. Their study was critical because there is a large variation in development speed of individual eggs. Eggs placed in the same incubator can vary in development from each other by a few HH stages due to a multitude of factors including, size, age of the hen laying the egg, age of the egg before incubation, and conditions the eggs were stored in before incubation. The breed of the egg also makes a difference in the speed of development.

In their staging guide, Hamburger and Hamilton showed that an embryo that has been incubating for 6 days can vary form HH Stage 27 to HH 31, and that lowering the temperature 2^{o} Celsius can cause embryos to skip "days" in development (Hamburger & Hamilton, 1992). Incubation temperatures 37.5^{o} C, 38^{o} C, and 39.4^{o} C were used for staging and different breeds of egg (White Leghorn, Barred Plymouth Rock, and Rhode Island Red) were compared at similar timepoints.

Stages 1-6 (0-25 hours of incubation) are known as the pre-somatic stages. That is, it is the stages of development before the formation of any somite pairs. Somites are blocks of mesoderm that form around the neural tube in vertebrate animals (DeRuiter 2010). They also determine the migratory path of neural crest cells in the early embryo. The early stages are distinguished by the formation and growth of the embryonic streak and the formation and growth of the notochord and headfold (Hamburger & Hamilton, 1992).

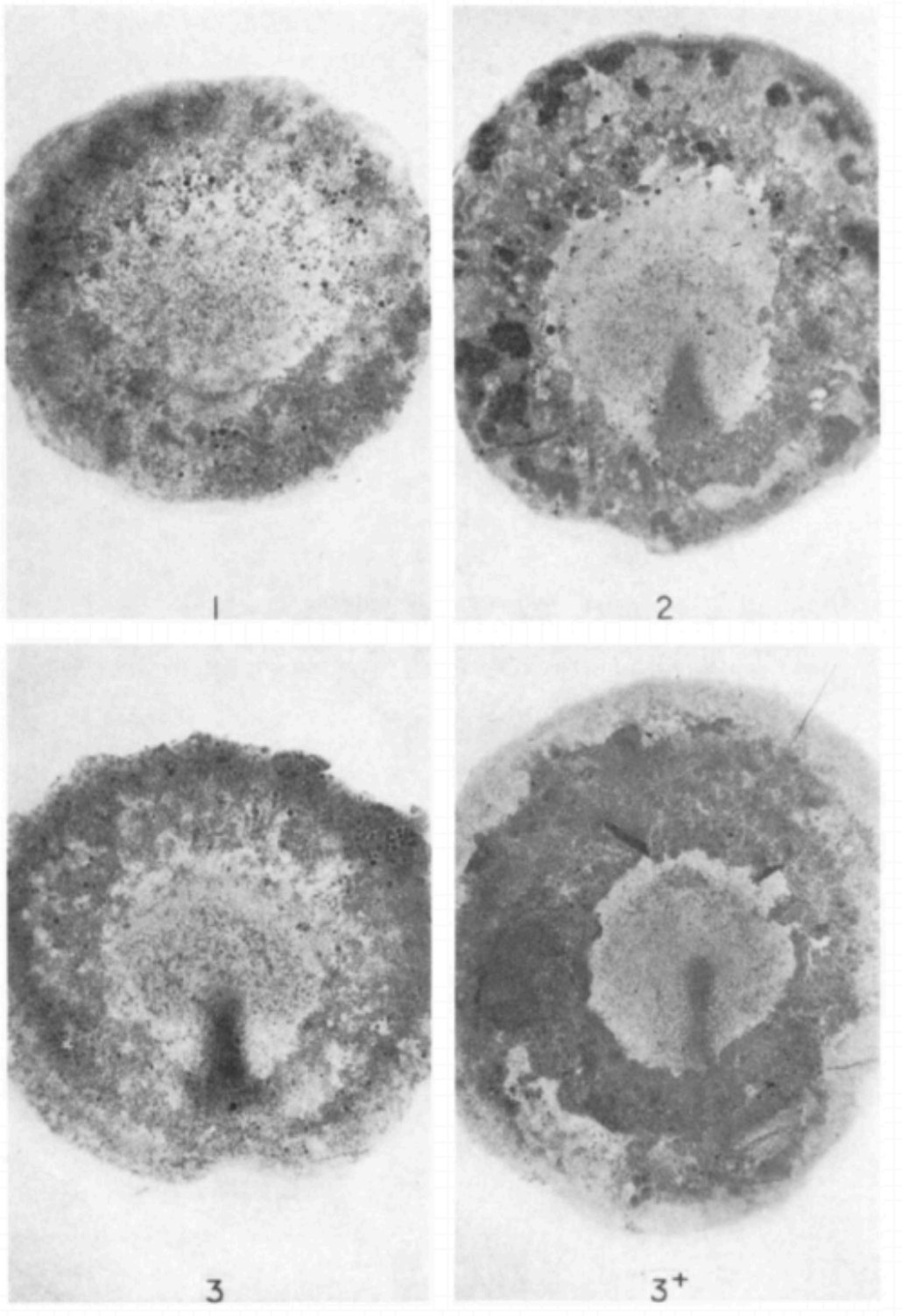

Figure 2.1. HH stages 1-3 are shown above. Stages 1-6 are characterized as the pre-somatic stage. The embryo consists only of the embryonic streak (Hamburger & Hamilton, 1992).

The next set of stages, HH 7-14, (23-43 hours of incubation at 37.5^{o} C) are characterized by the number of somites that the embryo has. Somite count grows from one somite at HH stage 7 to twenty-two somites at HH Stage 14. After HH 14, somites become hard to track and thus limb growth and development becomes the standard for tracking development. Wing and leg bud development, as well as beak shape are tracked from HH 14 to HH46 (20-21 days of incubation; newly hatched egg). One stage of interest in this study was HH 18 (~72 hours of incubation at 38^{o}C), the stage of surgical intervention. This is characterized as the last day that the outflow tract (OFT) is accessible for surgical intervention. The other stages of interest where extracellular matrix (ECM) development in the dorsal aorta, specifically elastin development, was observed was HH 36 (~10 days of incubation), HH 37 (~11 days of incubation), HH 39 (~13 days of incubation), HH 40 (~14 days of incubation), and HH 44 (~18 days of incubation) (Hamburger & Hamilton, 1992).

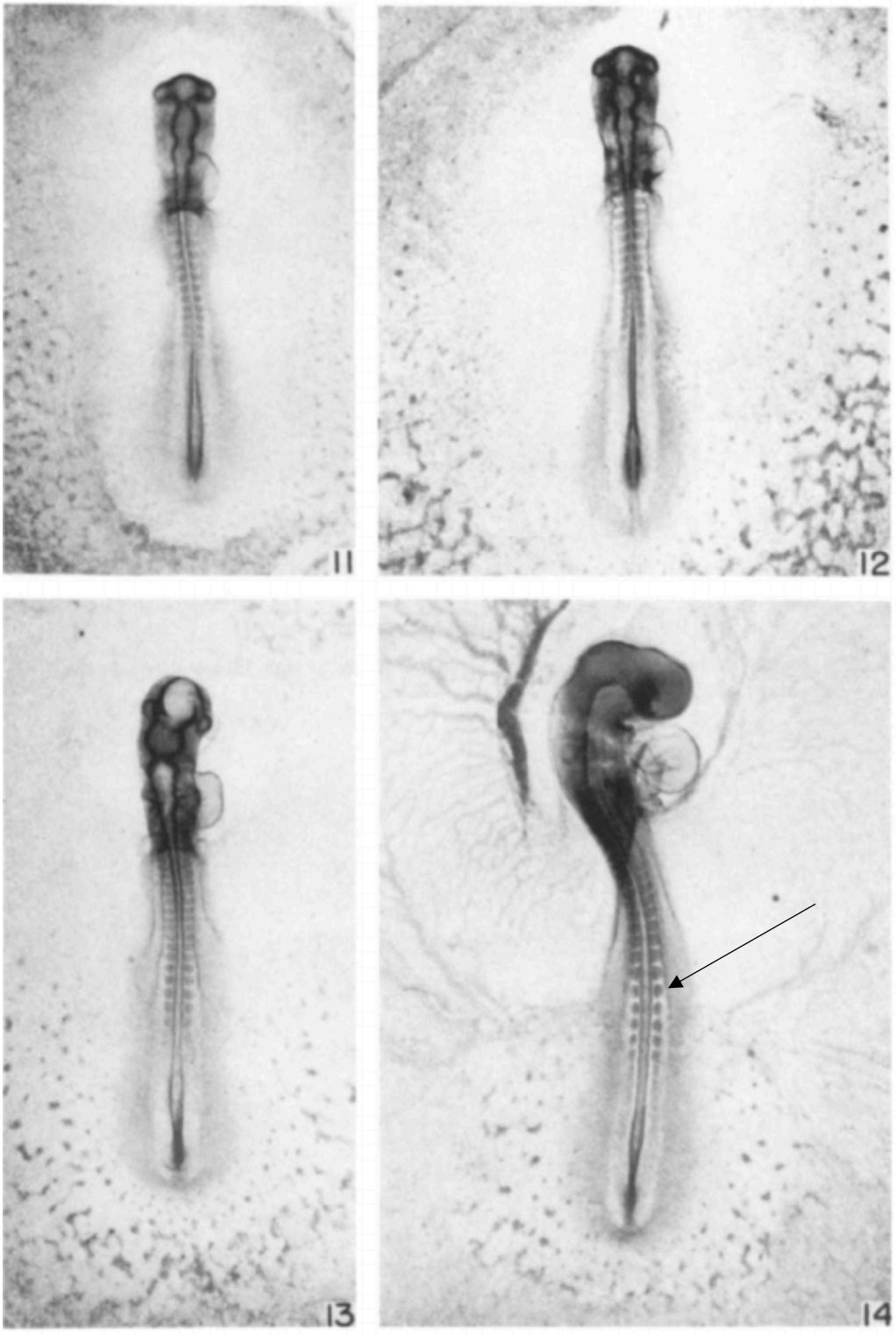

Figure 2.2. HH Stages 11-14 are shown above. Somite pairs are highlighted with the black arrow (Hamburger & Hamilton, 1992).

Because the OFT is being banded to study changes in hemodynamics and ECM development in this study, the OFT is of particular interest. The OFT is part of the original heart tube of the chick embryo, and connects the developing left ventricle to the arterial segments of the embryonic vascular system (Qayyum et al., 2001). It has been shown that the OFT has three endocardial cushions that are placed distally (away from the ventricle) and two that are placed proximally on the ventricle side of the OFT. The three distal cushions, along with two intercalated cushions are what give rise to the arterial valves as septation of the OFT occurs (Qayyum et al., 2001). Hemodynamics in the OFT are of particular interest, not only because early embryonic blood flow is key for development as discussed in Chapter 1, but it has been shown that changes in blood flow in the OFT affect stiffness properties of the endocardial tissues, affecting development of the embryonic heart and possibly arterial development. It was shown that increased hemodynamic load using OTB led to more collagen deposition in the OFT, which may lead to detrimental tissue remodeling as the OFT and the embryonic heart matures (Rennie et al., 2017). The flow pattern in the OFT has also been shown to be quite complex. Ultrasound imaging of the HH25 OFT shows a complicated flow pattern in the developing heart. Flow proceeded in the forward direction towards the dorsal aorta, and backwards towards the ventricle in a double helical fashion that may help drive septation of the OFT in the developing heart (Ho, Chan, Rajesh, Phan-Thien, & Yap, 2019).

Chapter 3: Surgical Interventions in Chick Embryos

There are many different surgical interventions that can be done in chick embryos. The most common surgical interventions are vitelline vein ligation (VVL), outflow tract banding (OTB), and left atrial ligation (LAL). Also, Vitelline artery ligation (VAL) is also done to study congenital heart disease. The surgical interventions are performed to analyze how changes in hemodynamics affect the formation of the early embryonic heart and study congenital heart disease mechanisms.

Almost 1% of newborns are born with some sort of congenital heart disease. Surgical intereventions on the early embryonic heart allow the study of how hemodynamics affect the formation of these malformations. Common heart defects include ventricular septal defects (VSD), pharyngeal arch malformations, atrio-ventricular/ semilunar valve malformation, double outlet right ventricle (DORV), and left heart hypoplasia (LHH) (Midgett & Rugonyi, 2014). In the figure below, Midgett and Rugonyi show the different placement of sutures for VVL, LAL, and OTB surgeries.

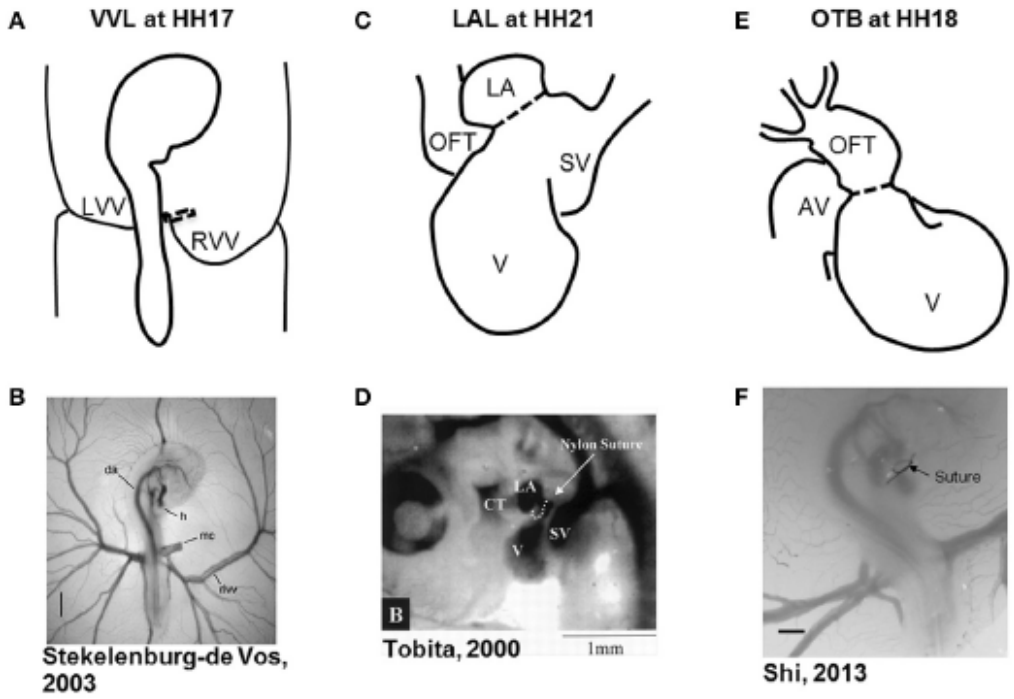

Figure 3.1. Comparison of three different surgical interventions. Ligations and restrictions are used to change the hemodynamics of the early embryonic heart to study formation of the heart and congenital heart disease (Midgett & Rugonyi, 2014).

In vitelline vein ligation ,or vitelline vein clipping- both produce the same effect, the left or right vitelline vein is ligated to redirect flow to the unligated vitelline vein. VVL is a good way to alter the flow patterns in the early cardiac system without altering drastically the volume of blood in the system. Hemodynamic changes with VVL are usually temporary, but the change in flow has been shown to start a remodeling cascade that leads to congenital heart defects (Midgett 2014). In another study, it was shown that VVL at HH18 leads to a decrease in peak flow velocity in the dorsal aorta by 49% (Espinosa et al., 2018). The blood flow then normalized to control values at HH19, followed by another reduction in aorta peak velocity of 32% at HH36. A decrease in elastin expression was seen in the arterial wall after VVL at HH34 and HH36. An increase in collagen expression was also seen at HH36. The decrease of flow through the dorsal

aorta at HH18 and HH36, along with the change in elastin and collagen expression over time is an example of how VVL can cause aortic remodeling over time.

Peak velocity is also perturbed in the dorsal aorta with VAL. It was shown that when VAL was done in HH21 chick embryos, an increase in pulse wave velocity (PWV), and peak proximal and peak distal aorta velocity was elevated in ligated embryos compared to control embryos (Lucitti, Visconti, Novak, & Keller, 2006). Increased aortic stiffness was observed in VAL embryos. The increased hemodynamics loads lead to an arterial wall with a threefold increase in collagen expression as a function of wall area fraction and an increase in the amount of smooth muscle α-actin (SMA) at HH27. Although more SMA-positive cells were seen in VAL embryos, the phenotype of those cells was less organized and immature compared to control embryos.

In OTB, the diameter of the OFT of the developing chick embryo is constricted with a suture. This constriction creates a local increase in peak velocity through the OFT. Wall shear rate at the site of banding increased with band tightness, or the level of constriction of the OFT, with a peak increase in velocity and wall shear rate through the OFT occurring around 40% band tightness (Midgett, Goenezen, & Rugonyi, 2014). Pressure also increases when the OFT is banded, with diastolic pressure, pulse transit time, and pulse pressure all increasing with band tightness (Shi 2013). An increase in dorsal aorta diameter was seen two hours after banding that was proportional to band tightness. Gene expression also changes with OTB. A decrease in cardiac cushion volume was seen when HH17 embryos were banded for 24 hours, as well as a significant decrease in the expression of the collagen1a1 gene (Menon, Eberth, Goodwin, & Potts, 2015).

While much work has been done to study the local effects of OTB on peak velocity, blood pressure, collagen expression, and the formation of cardiac defects, the downstream effects in the dorsal aorta have not been investigated. Specifically, the formation of the ECM, such as collagen and elastin has not been studied effectively. In this study, we hoped to study how the use of OTB affected the development of the embryonic dorsal aorta. We hoped to study changes in hemodynamics in the OFT and the DA, ECM development, and changes in arterial stiffness that accompanied the banding of the OFT over time.

Chapter 4: Methods

Chick Incubation

Fertilized chicken eggs were examined for cracks or other deficiencies. Cracked or severely soiled eggs were discarded and the rest were placed blunt side down in either a GQF Genesis 1588 Hova-Bator tabletop incubator or a QGF 1502 Digital Sportsman forced air incubator at 100º F (37.78º C) for 3 days until stage HH18 was reached. Eggs were then removed for surgical intervention and hemodynamic data gathering. They were then replaced back in the incubator for a maximum of 15 days- stage HH 44 (18 days of total incubation).

Outflow Tract Banding

Once embryos reached stage HH18, they were removed from the incubator. A 1 cm by 1cm section of shell was removed using a pair of fine forceps to puncture the shell and a pair of tweezers to remove the shell around the embryo. Embryos were then verified to be at HH18. If they were not at stage HH18, the hole in the shell was sealed with plastic cling wrap and put back in the incubator until stage HH18 was reached. Using a pair of dissection scissors and a pair of forceps, the membranes on top of the embryo were removed, allowing access to the embryonic heart. A length of 10-0 nylon monofilament suture was passed under the OFT of the heart and tied to constrict the OFT diameter. The suture was tied at various tightness level to achieve a spectrum of band tightness values. Eggs were then sealed in the manner above and placed back in the incubator or were taken for hemodynamic measurements.

OTB eggs were removed from the incubator 24 hours after initial surgery (stage HH 23), and the suture tied around the outflow tract was removed with care to ensure no bleeding occurred. If bleeding of the embryo occurred at any point of the surgery process, either during the initial surgery or when the suture was removed, the embryo was discarded.

Hemodynamic Flow Measurements

Hemodynamic measurements of the both outflow tract and the dorsal aorta were taken with ultrasound. The method was adapted from Tan et al. who used ultrasound to do a 3D reconstruction of the chick embryo vascular network (Tan, Jamil, Tee, Zhong, & Yap, 2015). A Vevo 2100 ultrasound system was used to gather hemodynamic data. The transducers used were the MS550D (22-55 Hz) and MS250 (13-24 Hz). The MS550D was used at earlier time points and the MS250 was used to collect data from older embryos. The embryo was covered with a plastic cling wrap (Saran Wrap), with the plastic touching the embryo. Warmed ultrasound gel was then placed on top of the plastic wrap to provide an imaging medium for the transducer. Eggs were then placed on a 3D translational stage with a heat lamp close to the stage shining on the embryo to keep the embryo at physiological temperatures. B-mode, M-mode, and Pulse wave velocity (PWV) mode data was collected to measure the degree of banding at the OFT and the velocity of blood flow through the OFT and the DA. Aorta velocity measurements were also taken at HH36 (10 days of incubation). Band tightness was calculated as:

$$1 - \frac{D_a}{D_b}$$

where D_b is the lumen diameter of the OFT before OTB and D_a is the lumen diameter of the OFT after OTB (Midgett 2014). WSR was calculated as:

$$WSR = 4\frac{v_c}{D}$$

where v_c is the centerline velocity of the OFT and D is the OFT diameter corresponding to the v_c measurement (Midgett 2014). Stroke Volume was calculated as:

$$SV = \frac{1}{2}A_c * VTI$$

where A_c is the cross-sectional area of the OFT and VTI is the velocity time integral of OFT flow measured using Doppler ultrasound (Phoon, Aristizábal, & Turnbull, 2002).

Embryo Dissection

Embryos were removed from their shell, decapitated, and the descending aorta was removed starting at just above the level of the heart. Dissections were performed for embryos at stages HH36, HH37, HH39, HH40, and HH44 (10, 11, 13, 14, and 18 days of Incubation). Time points were chosen to show the development of elastin over time and to see when mature arterial phenotypes became apparent. Heart weight and body weight measurements were taken at HH36.

Histology and Two Photon Microscopy

After embryos were dissected, descending aortas were fixed in a 4% Paraformaldehyde (PFA) solution for 24 hours. Aortas were then incubated in a sequential bath of 10%, 20%, and 30% sucrose, with each incubation being done overnight. After the sucrose protection, aortas were embedded in optical cutting temperature (OCT) medium. Vessels were sliced into 10µm slices using a cryostat, with cutting temperature set at -25^{o} C. Sections were then imaged using a Zeiss LSM 880 NLO two-photon microscope system. Sections were excited by a 680-1300 nm tunable laser set at 800nm. The signal collected in a Big 2 non-descanned detector (NDD) was split with a 760nm dichroic mirror and filtered by two bandpass filters, one for each channel. The two filters were in the range of 380-430nm (blue) and 580-670nm (red). The blue filter was used to collect second harmonic generation signal from collagen, and the red filter was used to collect the autofluorescence signal from elastin. Images were obtained using a 40x 1.3 NA oil objective.

Some PFA fixed aortas were instead sent to a histology core to be stained with hematoxylin and eosin (H&E) or Verhoeff-Van Gieson (VVG) stain. Samples were imaged under brightfield using a 20x objective.

Chapter 5: Results

Hemodynamic Changes Due to OTB Intervention

Hemodynamic measurements at HH18 compared the flow characteristics in the OFT and the DA before and after OTB intervention. Band tightness was measured from change in lumen diameter measured from M-mode images taken using pulse-wave Doppler ultrasound. Band tightness ranged from 4.4% to 74.4%. Peak velocity in the OFT was measured before and after to measure the effect of band constriction on blood flow in the OFT. Flow in the OFT had a parabolic-like flow pattern versus band tightness with max velocity seen with a band tightness between 30% and 40% band tightness as seen in Figure 5.1. The same flow pattern was exhibited by the net increase in flow seen after OTB. Flow velocity in the OFT after intervention varied from 55.80 mm/s to 144.04mm/s. Maximum increase in flow velocity after intervention was 80.86 mm/s.

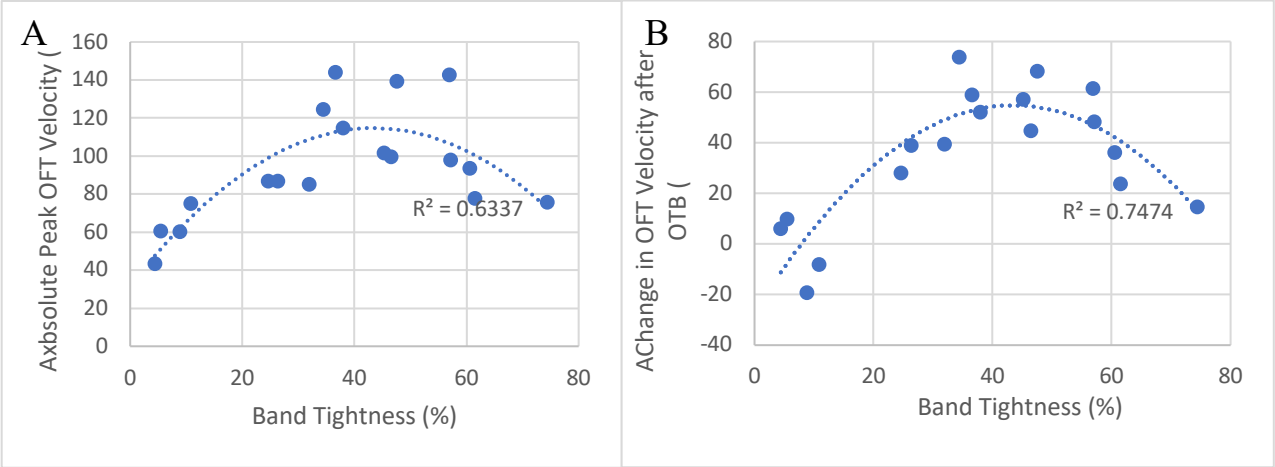

Figure 5.1. The effect of OTB intervention on OFT peak velocity. Both the absolute velocity (a) and the change in velocity (b) are shown above. The change in OFT velocity was parabolic-like and the maximum increase in velocity was seen at around 40% band tightness. R^2 values were 0.633 and 0.747 respectively. R^2 values show the quality of the parabolic fits to the data. The closer R^2 values are to one, the better the parabolic fit.

Average flow velocity in the OFT before and after OTB was compared to determine if there was a significant difference between the two groups. One-way ANOVA showed that the average values between the two groups were statistically significant ($P= 2.05*10^{-9}$). Average blood velocity before intervention in the OFT was 59.62 mm/s and 94.81 mm/s after intervention.

Velocity in the DA was also measured before and after OTB at HH18. A linear-like decrease in velocity was observed in the DA as band tightness increased. An increase in DA velocity was seen until 10% band tightness. A decrease in DA velocity was seen with band tightness after 20% band tightness, suggesting that there is a critical point after which DA velocity does not increase, but rather decreases with band tightness. DA velocity varied from 58.21 mm/s to 15.31 mm/s with increasing band tightness as shown in Figure 5.2. Average DA velocity before intervention was 46.13 mm/s and 38.61 mm/s after intervention (P=.018).

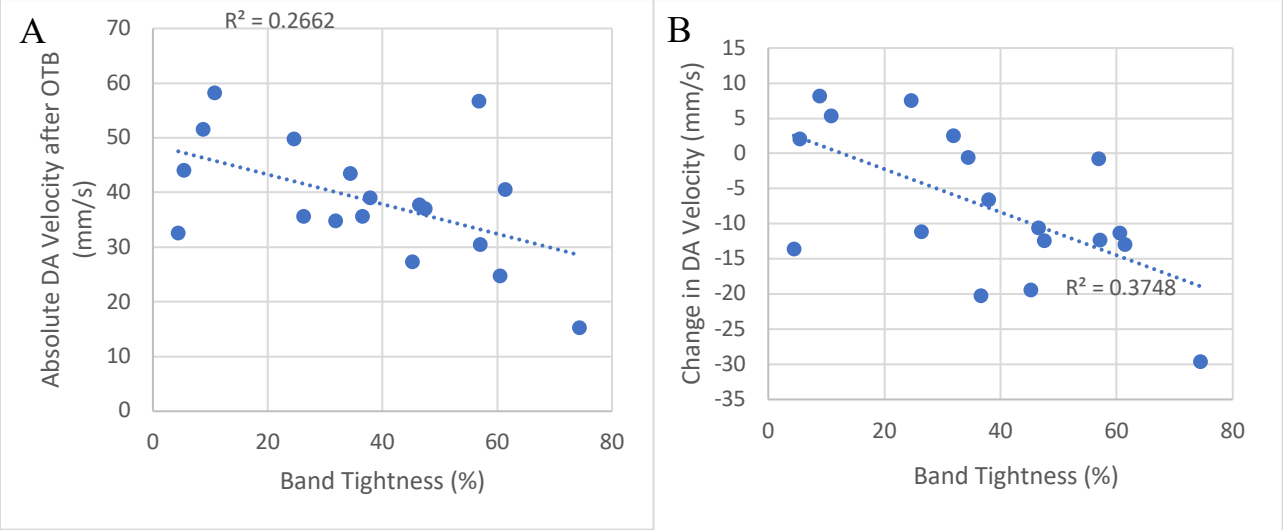

Figure 5.2. The effect of OTB intervention on DA velocity before and after intervention. In both the absolute DA velocity (a) and the change in DA Velocity (b), an increase in velocity was followed by a linear-like decrease in velocity with respect to increasing band tightness. Maximum DA velocity was seen at around 10% band tightness. R^2 values were 0.266 and 0.375 respectively. R^2 values show the quality of the linear fits to the data. The closer R^2 values are to one, the better the linear fit.

Wall Shear Rate (WSR) was calculated in the OFT before and after intervention. WSR after intervention showed a linear-like increase in value with respect to band tightness. The same pattern was observed for the net change in WSR. Average WSR before intervention at HH18 was 276.15 s^{-1} and was 820.24 s^{-1} after intervention. The average values were significantly different showing that OTB changes the flow pattern in the OFT, causing at least a local perturbation in the flow through the early cardiac unit ($P= 4.84*10^{-5}$).

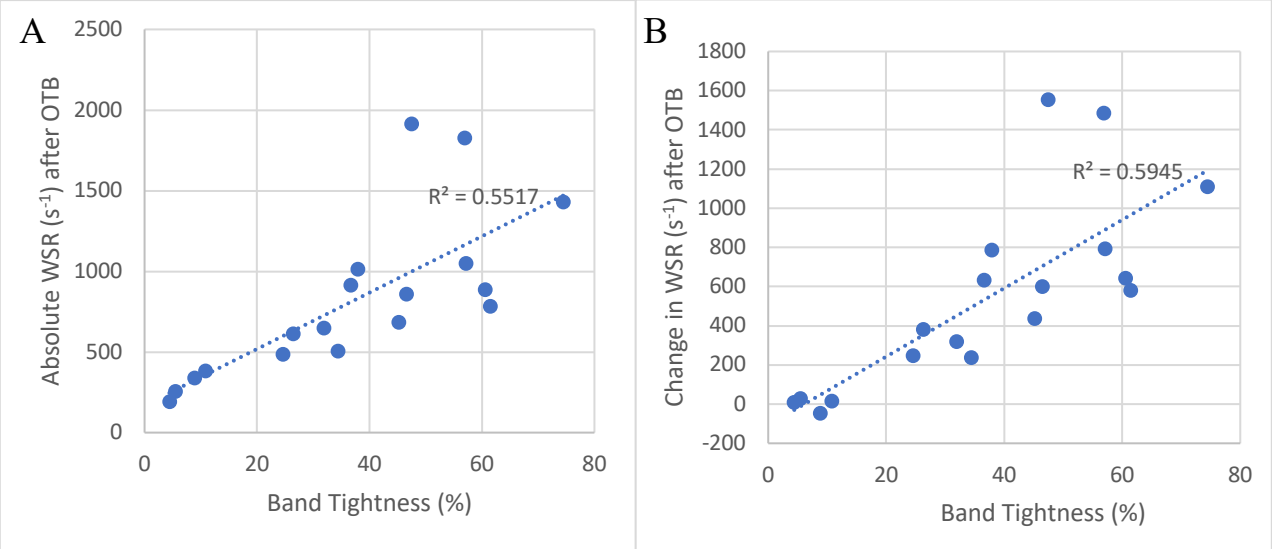

Figure 5.3. Wall Shear Rate after OTB intervention. The absolute increase in WSR (a) and the net change in WSR (b) in the OFT both exhibit a linear-like increase with increasing band tightness, showing the increased hemodynamic load exhibited by the OFT due to OTB intervention. R^2 values show the quality of the linear fits to the data. R^2 values 0.552 and 0.594 respectively. The closer R^2 values are to one, the better the linear fit.

Stroke Volume through the OFT at HH18 before and after OTB was also recorded. Average velocity flow values were used instead of peak velocity values in the OFT. There was a decrease in stroke volume after OTB intervention compered to before intervention. A clear pattern was not discernable; however, average SV after OTB was significantly lower than SV before OTB as seen in Figure 5.4 below ($P=4.81*10^{-9}$). The average stroke volume before

intervention was 1.25 mm^3/beat and the average stroke volume after intervention was calculated to be 0.48 mm^3/beat.

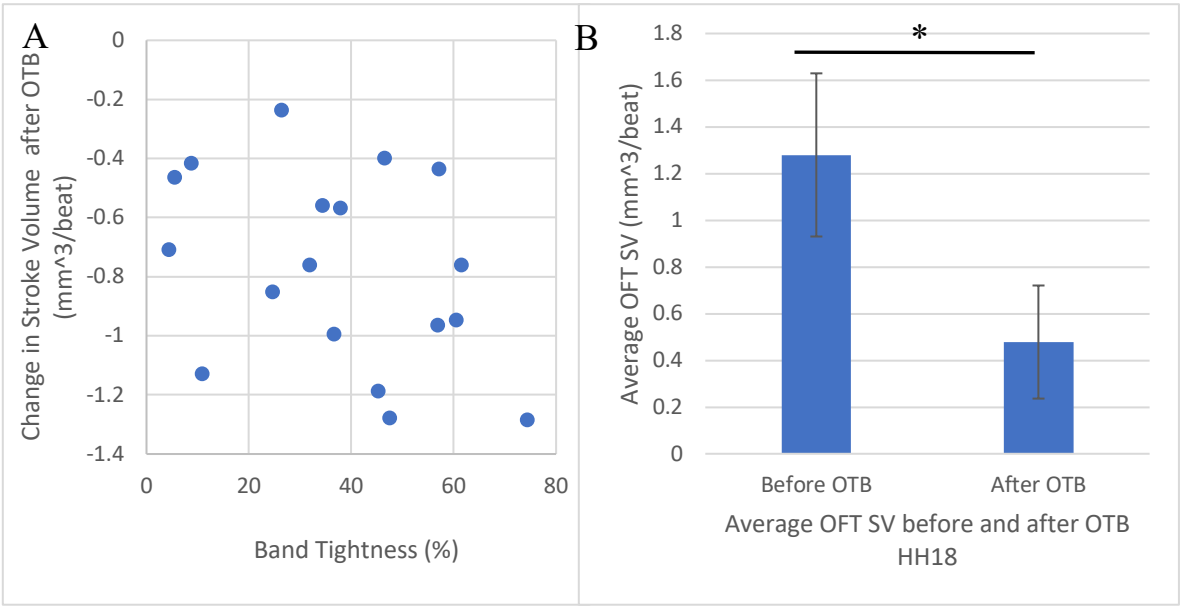

Figure 5.4. The change in stroke volume due to OTB intervention. No discernable pattern of decrease in SV was seen with an increase in band tightness (a); however, SV after OTB was significantly lower that before OTB (b).

Average OFT velocity, DA velocity, and OFT diameter at HH23 were also measured. Average OFT velocity was measured at HH23 before and after the suture was removed. The average OFT velocity with the suture on was 161.15mm/s and the average OFT velocity after removing the suture was 121.46 mm/s as seen below in Figure 5.5. The values OFT were not significantly different before and after removing the suture. Average DA velocity was also measure before and after suture removal at HH23. The average velocity of blood through the DA was 53.35mm/s and was 61.80 mm/s after suture removal. OFT diameter was also measured before and after suture removal. Average OFT diameter with the suture on was 0.21mm and was 0.31mm after suture removal. The change in OFT lumen diameter before suture removal compared to after suture removal was found to be statistically significant (P=.045). The change

in DA velocity before suture removal compared to after suture removal was not statistically significant.

Average DA velocity at HH36 was also measured for control embryos and OTB embryos. The average DA velocity for control embryos was found to be 226.2mm/s and DA velocity in OTB embryos was found to be 191.07mm/s. The values between the two groups were determined to be not significantly different from one another, suggesting that as time goes on, the hemodynamics of the OTB group starts to recover from load changes due to surgical intervention.

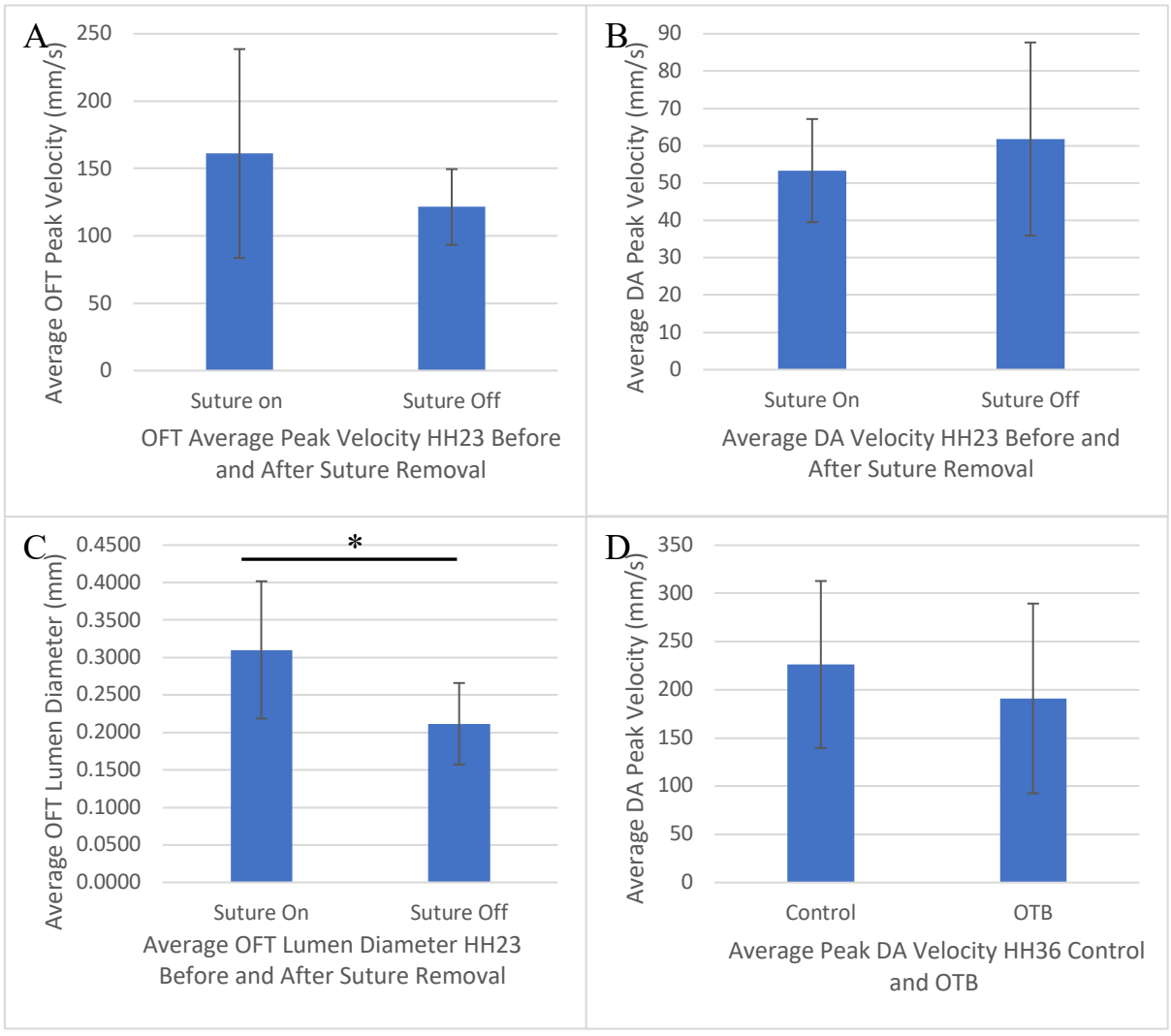

Figure 5.5. Average flow properties for HH23 and HH36 are shown above. Average peak OFT blood velocity (a) and average peak DA velocity (b) for HH23 shown. A slight decrease in OFT velocity and slight increase in DA velocity is observed with suture removal. OFT lumen diameter is also shown before and after suture removal (c) at HH23. Lumen diameters between the two groups at HH23 were significantly different. Average peak DA velocity for control and OTB groups at HH36 (d) is also shown

Two Photon Images

Two photon images were taken of control and OTB DA cross-sections. Images were taken at HH36, HH37, HH39. Control DA cross-sections were also imaged for HH40 and HH44. Collagen was captured on the cyan channel and elastin on the magenta channel in Figure 5.6.

Two-photon images taken at HH36 showed little to no collagen or elastin structure. There were no visible elastic lamina. Early collagen structure was apparent by HH36 onward, however collagen development was inconsistent at early time points (HH36, HH37). The same phenomenon was seen at HH37. Collagen structure started to become apparent at HH39, and elastin structure first started to become apparent at HH40. Mature collagen and elastin structure started to become apparent at HH44; however, elastin did not show a mature phenotype. Instead, the emergence of fiber strands was apparent at HH40, but no full lamina had formed. Mature aortic wall phenotypes had not formed 2-3 days from hatching, suggesting that most arterial wall development occurs in the few days before birth.

Histology sections of H&E and VVG were taken for HH36 and HH37 control and OTB showing little to no elastin formation. Cell nuclei were present with H&E staining.

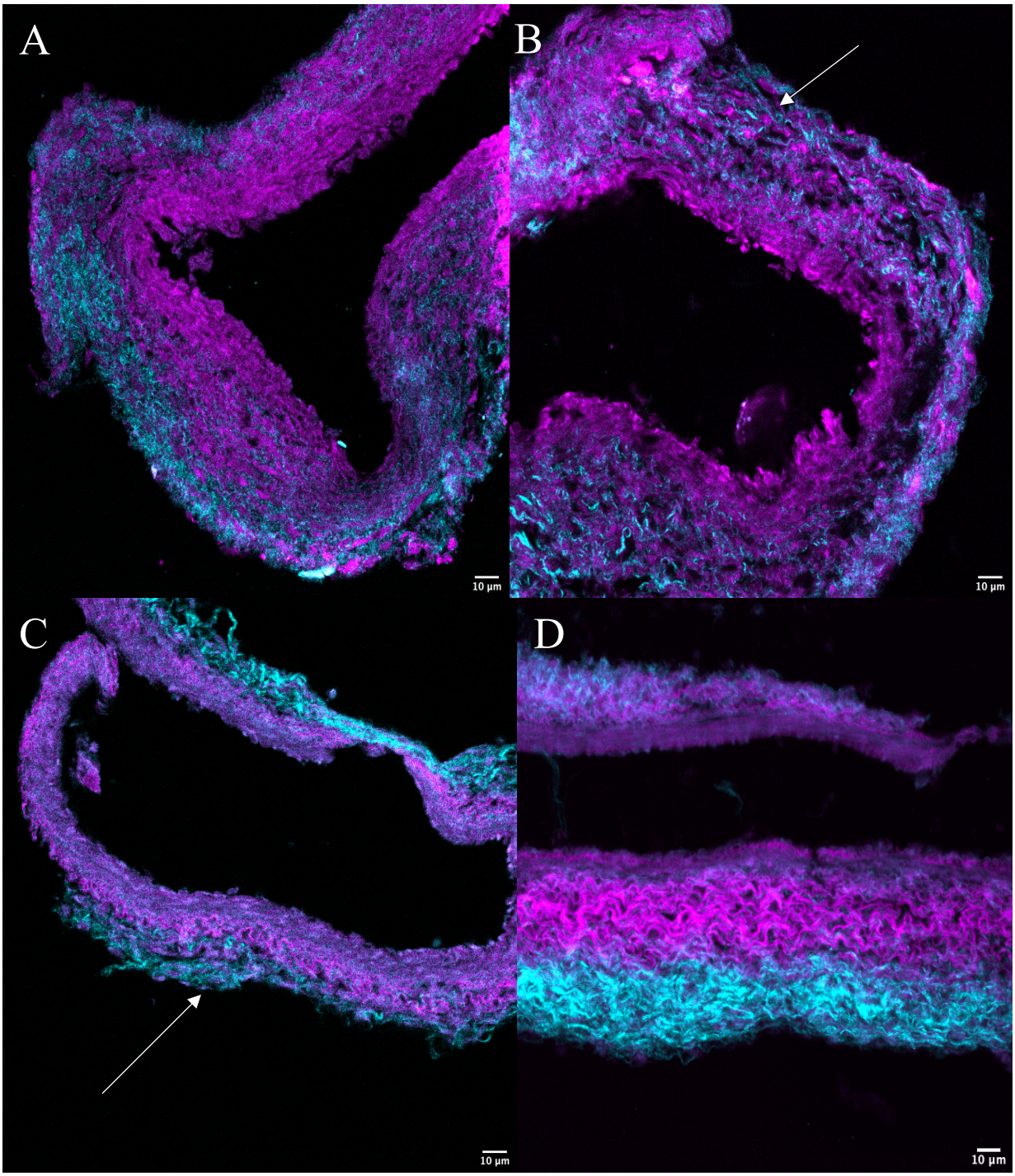

Figure 5.6. Two photon images of a HH37 control (a), HH39 OTB (b), HH40 control (c), and HH44 control (d), dorsal aortas are shown above. Collagen is shown in cyan and elastin in magenta. No difference was seen between OTB and control phenotypes for collagen and elastin. HH36 and HH37 OTB and control aortas all resembled the aorta shown in (a). Clumps of Elastin are seen forming by HH39 (white arrow in (b)). Elastin fibers started to form by HH40 (white arrow in (c)). By HH44, large elastin fibers had started to form, yet no complete lamina had formed.

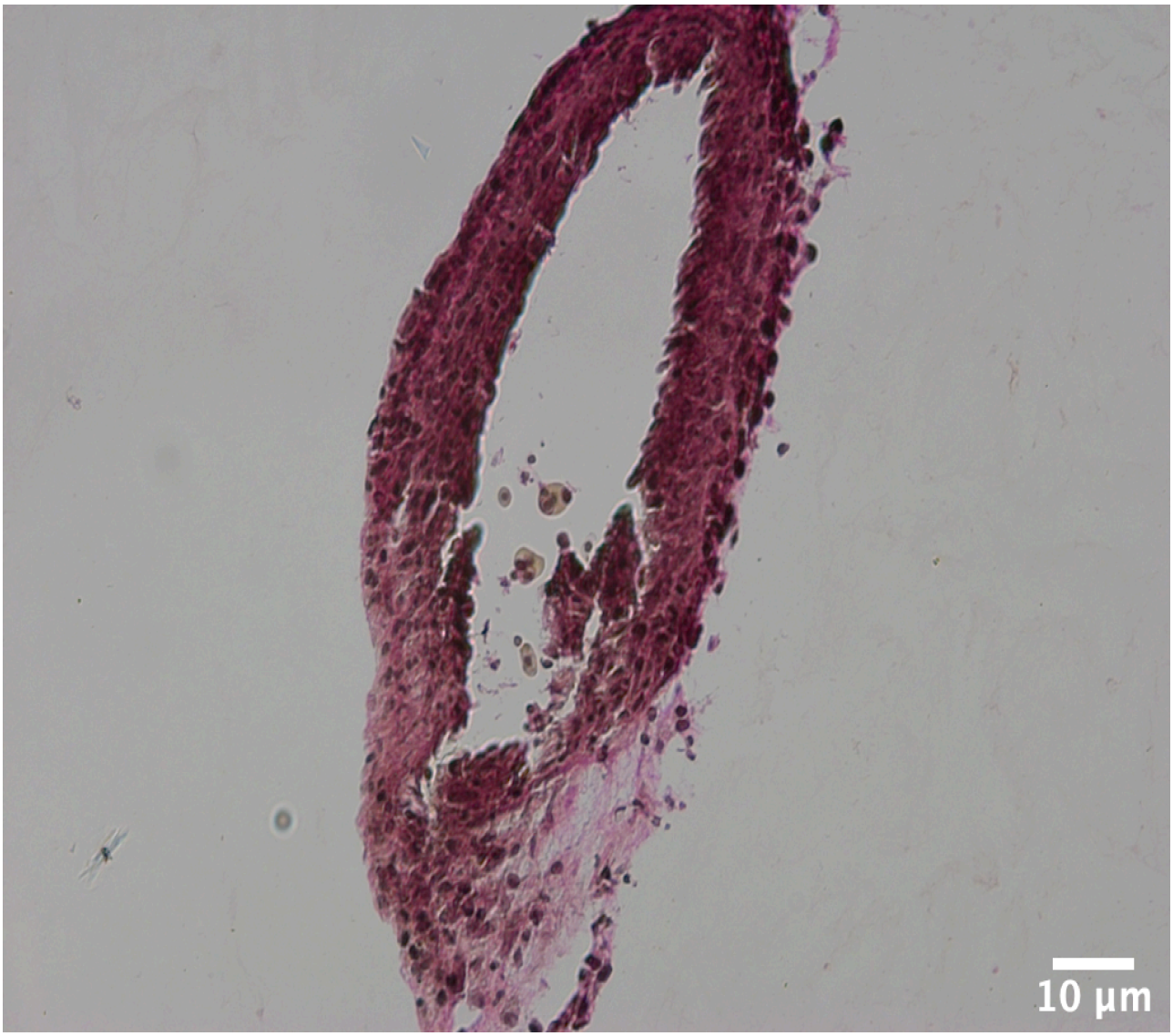

Figure 5.7. VVG Stain of HH36 OTB DA. Black dots represent cell nuclei. Very little if no elastin can be seen through histological staining.

Chapter 6: Discussion

OTB and local blood velocities

The velocity profile in the OFT after OTB banding was found to have a parabolic-like pattern, with the maximum OFT velocity centered around 40% band tightness. This pattern of parabolic flow in the OFT due to OTB agrees with previous findings that have shown similar results (Rugonyi, Shaut, Liu, Thornburg, & Wang, 2008). There has been relatively little data collected about changes in DA hemodynamics, and no data collected about the effect that OTB has on the hemodynamics of the DA during embryonic development. As stated above, Espinosa et al. reported that VVL causes a decrease in DA velocity leading to a reported decrease in elastin content at HH36. Lucitti et al. also reported that that VAL at HH21 (Day 3.5) causes a decrease in the time-average velocity, and peak proximal and distal velocity at HH21, HH24, and HH27 a global decrease in arterial compliance (Lucitti et al., 2006). They reported that the decrease in DA velocity and compliance was due to increased hemodynamic load due to VAL.

While conducting experiments, the original hypothesis was that since OFT sees an increase in local velocity due to OTB, assuming SV stayed the same, an immediate increase in DA velocity would be seen. While the expected increase in OFT velocity was seen, the linear like increase in WSR and decrease in SV were not expected based on the literature. Midgett et al. reported a parabolic pattern of WSR versus band tightness following the same pattern of peak OFT velocity versus band tightness that was previously reported. SV was also reported to be relatively constant by Midgett et al.; however, we observed a decrease in SV with increasing band tightness. Although not consistent with Midgett et al., a decrease in DA velocity coupled with a decrease in SV is consistent with the decrease in velocity and compliance seen in the DA that was reported by Lucitti et al. due to increased hemodynamic load. Because band tightness

values up to 10% saw an increase in DA velocity, it seems that there is a small range of band tightness values than can cause a small enough increase in hemodynamic load that an increase in DA velocity can be seen.

One interesting observation was that average OFT diameter decreased after suture removal, opposite to the hypothesis that OFT diameter would return to values similar to control embryos due to the removal of the constricting band around the OFT. This reduction in diameter might be explained by the early cardiac system's attempt to maintain a constant pressure in the system in response to changes in hemodynamic load.

OTB can be used to alter DA velocity, likely responding to the hemodynamic stress added to the system by surgical intervention. Small constrictions in the OFT lumen diameter can lead to an increase in both OFT and DA velocities. However, past 10% constriction, DA velocity starts to decrease and eventually will become smaller than control values. For values where DA velocity is smaller than control values, aortic development will likely lag behind that of control aortas in response to less blood flow to the DA due to decreased SV and peak velocity.

DA development and ECM deposition

Two photon images were enlightening by showing that elastin development and deposition occurs at a much slower process than thought otherwise. Elastin auto-fluorescence images taken at HH36 and HH37 showed little to no elastin clumps or fiber formation in the arterial wall. Elastin production in the early chick embryo has been shown to begin at after 5.5-6 days of incubation (HH27) (El-Maghraby & Gardner, 1972). However, elastin clumps were seen at HH39 and elastin deposition into fibers was not seen until HH44. It may be that autofluorescent signal depends on denser, larger elastin aggregates or fibers than previous studies that used antibodies. The formation of elastin aggregates and the late formation of elastin fibers

is consistent with previous studies of elastin biosynthesis in chick embryos (Arciniegas, Servin, Argüello, & Mota, 1989; Damiano, Tsang, Weinbaum, Christner, & Rosenbloom, 1984). Yamazaki et al. showed that elastogenesis and fibrillin deposition were detected at embryonic day (ED) 4 in the aortic wall. Elastin content was significantly less than fibrillin content and elastin deposition into the ECM occurred significantly later in chick embryonic development (Yamazaki, Sejima, Yuguchi, Namba, & Isokawa, 2007). They also showed that elastin fibers forming around an amorphous core at day 17 (HH43). The late deposition of elastin into fibers was seen in the two-photon images in Figure 5.6. Aortic cross-sections of HH36 and HH37 embryos showed little to no mature elastin was seen in the wall. Elastin fiber formation was only present in images taken at HH44, reinforcing the idea that elastin formation occurs later in the gestation period. To further study the effects of increase hemodynamic load on arterial development, it is necessary to look further in the embryonic cycle. Most of elastin fiber formation has been seen to happen in the last 3-4 days before hatching.

Challenges with egg viability

Incubation temperature is the most important factor for ensuring optimal incubation of chick embryos. As reported earlier, optimal incubation can vary anywhere from 37^{o}C to 39.4^{o}C as reported in the Hamburger Hamilton Stages. If incubator temperature is kept too low, eggs will develop at a slower rate that the standard rates listed in the Hamburger Hamilton stages. If incubator temperature is set too high, embryos will develop too quickly. In both cases, usually the growth rate, whether delayed or increased, will be unsustainable and the embryos will eventually die. Initially, while trying to collect data, the incubator in use had multiple issues keeping a constant temperature and humidity. Efforts to calibrate and correct the temperature were not successful. Also, the incubator in question would spring leaks and from the water pan

and drown the embryos, killing them. The incubator had to be replaced for one with digital controls. A digital control center is the easiest way to ensure that proper incubator temperature is being maintained. Once a new incubator was in use, constant incubator could be maintained easily.

Another factor that determines the viability of the eggs is the age of the eggs that are used for incubation. It is best if the eggs that are used for incubation are as close to the date of laying and fertilization as possible. The longer the time between the laying of the egg to the start of incubation, the weaker the health of the embryo will be once incubation starts. It was found that if older eggs were used for incubation (eggs older than one week from laying), a developmental lag would be seen. On average, a developmental lag of 6-12 hours was seen from the average incubation times necessary to reach given stages in the Hamburger Hamilton stages.

The third factor that impaired the viability of the eggs used for incubation was the manner in which eggs were transported from their laying point to the laboratory for use. Eggs were sourced from many different sources in order to find the optimal provider of fertilized eggs. Air transport and ground transport were used in an effort to receive the eggs in the best condition as possible. Eggs were often cracked, damaged, and exposed to extreme fluctuations in temperature. Eggs shipped in the summer months would die from heat, and eggs in the winter would die from the cold. Often, lack of care by delivery services would cause the most harm, and any attempts to ensure that proper care was being taken by delivery services would be ignored. Because of the massive effect egg quality (age and the manner in which eggs were delivered) had on the ability to conduct experiments, multiple different egg sources were tried, including universities and farms. Often the best viability rate that could be achieved, due to the multiple factors listed above, was around 50%. We ended up using a farmer in Oregon as the source for

most of the eggs in this study. That provided consistent quality eggs, but shipping conditions still reduced viability in some cases. To solve the problems listed above, it would be ideal to have direct access to a local hen and rooster breeder pair so that variables of egg age and quality could be identified and controlled for and shipping was not necessary. The practicality of such a solution is left up to each individual investigator.

Challenges with surgical intervention

Apart from issues with egg quality and incubation, surgical interventions themselves introduce major hurdles in time-based or developmental studies. It has been shown that OTB causes a decrease in the survivability**.** The average survivability of control embryos to HH38 (Day 12) was shown to be around 50%, with OTB groups having around a 38% survivability to HH38 for 10-45% band tightness (Midgett et al., 2017). The lowest survivability rates were associated with the highest peak velocities after banding in the OFT. The effect OTB has on survivability becomes increasingly important as it seems that the best way to study the effects that OTB has on elastin development is to incubate embryos as close to hatching as possible. The best way to combat the decrease in survivability seen with OTB embryos is to use a large amount of eggs to collect data as it is virtually guaranteed that survivability rates will be lower for OTB, or any surgical intervention group than control embryos.

Conclusions and future work

OTB was shown to locally increase the peak blood velocity of OFT and decrease the peak DA velocity immediately after banding at HH18. Removing the suture 24 hours after banding led to hemodynamic values that were similar to control values. By HH36, no significant difference in DA velocity was seen between control and OTB embryos.

The decrease in DA velocity is likely in response to perturbation caused in the early cardiac system due to OTB similar to the decrease in velocity seen in VAL and VVL as discussed above. This decrease in velocity will likely lead to aortic phenotypes that are less developed than their control counterparts similar to phenotypes seen by Lucitti et al. discussed above. Shi et al., as discussed previously, also witnessed an increase in DA diameter after OTB intervention, giving more evidence that OTB puts stress on the early cardiac system, delaying downstream development in the DA (Shi et al., 2013). The decrease in SV was interesting as to imply that the amount of blood circulating in the early cardiac system was reduced. This is something that has not been observed before and could be the reason that DA velocity is decreased. Early ventricle flow properties, as well as early ventricle dimensions in response to OTB should reveal if more blood is staying in the ventricle, reducing the efficiency of the early embryonic heart.

This delay in development may be observed seen through changes in elastin fiber synthesis. OTB aortas should be delayed in expressing elastin fibers, something that should be seen around HH43 or HH44.

To confirm that OTB delays DA development, it is necessary to measure the pressure in the primitive ventricle and DA before and after OTB at HH18. This will help confirm SV values that were calculated in this study. Also, pressure values in the DA coupled with DA diameter measurement before and after OTB will help determine if the decrease in DA velocity is an effort to keep pressure in the system constant. Two-photon images between groups starting at HH39 onwards should give an insight if elastin is indeed delayed in forming fibers as hypothesized.

References

Arciniegas, E., Servin, M., Argüello, C., & Mota, M. (1989). Development of the aorta in the chick embryo: structural and ultrastructural study. *Atherosclerosis*, *76*(2–3), 219–235. https://doi.org/10.1016/0021-9150(89)90106-8

Breckenridge, R. (2010, March 1). Heart failure and mouse models. *Disease Models and Mechanisms*, Vol. 3, pp. 138–143. https://doi.org/10.1242/dmm.005017

Damiano, V., Tsang, A. L., Weinbaum, G., Christner, P., & Rosenbloom, J. (1984). Secretion of Elastin in the Embryonic Chick Aorta as Visualized by Immunoelectron Microscopy. *Topics in Catalysis*, *4*(2), 153–164. https://doi.org/10.1016/S0174-173X(84)80022-9

El-Maghraby, M. A. H. A., & Gardner, D. L. (1972). Development of connective-tissue components of small arteries in the chick embryo. *The Journal of Pathology*, *108*(4), 281–291. https://doi.org/10.1002/path.1711080404

Espinosa, M. G., Taber, L. A., & Wagenseil, J. E. (2018). Reduced embryonic blood flow impacts extracellular matrix deposition in the maturing aorta. *Developmental Dynamics*, *247*(7), 914–923. https://doi.org/10.1002/dvdy.24635

Gilbert, S. (2000). *Developmental Biology* (6th ed.). Retrieved from https://www.ncbi.nlm.nih.gov/books/NBK9974/#_A52_

Hamburger, V., & Hamilton, H. L. (1992). A series of normal stages in the development of the chick embryo. *Developmental Dynamics*, *195*(4), 231–272. https://doi.org/10.1002/aja.1001950404

Ho, S., Chan, W. X., Rajesh, S., Phan-Thien, N., & Yap, C. H. (2019). Fluid dynamics and forces in the HH25 avian embryonic outflow tract. *Biomechanics and Modeling in Mechanobiology*, *18*(4), 1123–1137. https://doi.org/10.1007/s10237-019-01132-6

Hoffman, J. I. E., & Kaplan, S. (2002, June 19). The incidence of congenital heart disease. *Journal of the American College of Cardiology*, Vol. 39, pp. 1890–1900. https://doi.org/10.1016/S0735-1097(02)01886-7

Hove, J. R., Köster, R. W., Forouhar, A. S., Acevedo-Bolton, G., Fraser, S. E., & Gharib, M. (2003). Intracardiac fluid forces are an essential epigenetic factor for embryonic cardiogenesis. *Nature*, *421*(6919), 172–177. https://doi.org/10.1038/nature01282

Li, Y. S. J., Haga, J. H., & Chien, S. (2005, October 1). Molecular basis of the effects of shear stress on vascular endothelial cells. *Journal of Biomechanics*, Vol. 38, pp. 1949–1971. https://doi.org/10.1016/j.jbiomech.2004.09.030

Lucitti, J. L., Visconti, R., Novak, J., & Keller, B. B. (2006). Increased arterial load alters aortic structural and functional properties during embryogenesis. *American Journal of Physiology - Heart and Circulatory Physiology*, *291*(4), 1919–1926. https://doi.org/10.1152/ajpheart.01061.2005

Ma, Z. H., Ma, Y. S., Zhao, Y. Q., Liu, J. H., Liu, J. H., Lv, J. T., & Wang, Y. (2017). Measurement of the absolute velocity of blood flow in early-stage chick embryos using spectral domain optical coherence tomography. *Applied Optics*, *56*(31), 8832–8837. https://doi.org/10.1364/AO.56.008832

Menon, V., Eberth, J., Goodwin, R., & Potts, J. (2015). Altered Hemodynamics in the Embryonic Heart Affects Outflow Valve Development. *Journal of Cardiovascular Development and Disease*, *2*(2), 108–124. https://doi.org/10.3390/jcdd2020108

Midgett, M., Goenezen, S., & Rugonyi, S. (2014). Blood flow dynamics reflect degree of outflow tract banding in Hamburger-Hamilton stage 18 chicken embryos. *Journal of the Royal Society Interface*, *11*(100). https://doi.org/10.1098/rsif.2014.0643

Midgett, M., & Rugonyi, S. (2014). Congenital heart malformations induced by hemodynamic altering surgical interventions. *Frontiers in Physiology*, *5 JUL*(August), 1–18. https://doi.org/10.3389/fphys.2014.00287

Midgett, M., Thornburg, K., & Rugonyi, S. (2017). Blood flow patterns underlie developmental heart defects. *American Journal of Physiology - Heart and Circulatory Physiology*, *312*(3), H632–H642. https://doi.org/10.1152/ajpheart.00641.2016

Olesen, S. P., Claphamt, D. E., & Davies, P. F. (1988). Haemodynamic shear stress activates a K+ current in vascular endothelial cells. *Nature*, *331*(6152), 168–170. https://doi.org/10.1038/331168a0

Phoon, C. K. L., Aristizábal, O., & Turnbull, D. H. (2002). Spatial velocity profile in mouse embryonic aorta and Doppler-derived volumetric flow: a preliminary model. *American Journal of Physiology-Heart and Circulatory Physiology*, *283*(3), H908–H916. https://doi.org/10.1152/ajpheart.00869.2001

Qayyum, S. R., Webb, S., Anderson, R. H., Verbeek, F. J., Brown, N. A., & Richardson, M. K. (2001). Septation and valvar formation in the outflow tract of the embryonic chick heart. *The Anatomical Record*, *264*(3), 273–283. https://doi.org/10.1002/ar.1162

Rennie, M., Stovall, S., Carson, J., Danilchik, M., Thornburg, K., & Rugonyi, S. (2017). Hemodynamics Modify Collagen Deposition in the Early Embryonic Chicken Heart Outflow Tract. *Journal of Cardiovascular Development and Disease*, *4*(4), 24. https://doi.org/10.3390/jcdd4040024

Rugonyi, S., Shaut, C., Liu, A., Thornburg, K., & Wang, R. K. (2008). Changes in wall motion and blood flow in the outflow tract of chick embryonic hearts observed with optical coherence tomography after outflow tract banding and vitelline-vein ligation. *Physics in*

Medicine and Biology, *53*(18), 5077–5091. https://doi.org/10.1088/0031-9155/53/18/015

Sedmera, D., Pexieder, T., Rychterova, V., Hu, N., & Clark, E. B. (1999). Remodeling of chick embryonic ventricular myoarchitecture under experimentally changed loading conditions. *The Anatomical Record*, *254*(2), 238–252. https://doi.org/10.1002/(SICI)1097-0185(19990201)254:2<238::AID-AR10>3.0.CO;2-V

Shi, L., Goenezen, S., Haller, S., Hinds, M. T., Thornburg, K. L., & Rugonyi, S. (2013). Alterations in pulse wave propagation reflect the degree of outflow tract banding in HH18 chicken embryos. *American Journal of Physiology - Heart and Circulatory Physiology*, *305*(3), 386–396. https://doi.org/10.1152/ajpheart.00100.2013

Stewart, D. E., Kirby, M. L., & Sulik, K. K. (1986). Hemodynamic Changes in Chick Embryos Precede Heart Defects After Cardiac Neural Crest Ablastion. Retrieved April 10, 2020, from Circulation Research website: https://www.ahajournals.org/doi/pdf/10.1161/01.RES.59.5.545

Tan, G. X. Y., Jamil, M., Tee, N. G. Z., Zhong, L., & Yap, C. H. (2015). 3D Reconstruction of Chick Embryo Vascular Geometries Using Non-invasive High-Frequency Ultrasound for Computational Fluid Dynamics Studies. *Annals of Biomedical Engineering*, *43*(11), 2780–2793. https://doi.org/10.1007/s10439-015-1339-y

Tobita, K., & Keller, B. B. (2000). Right and left ventricular wall deformation patterns in normal and left heart hypoplasia chick embryos. *American Journal of Physiology - Heart and Circulatory Physiology*, *279*(3 48-3). https://doi.org/10.1152/ajpheart.2000.279.3.h959

Tobita, K., Schroder, E. A., Tinney, J. P., Garrison, J. B., & Keller, B. B. (2002). Regional passive ventricular stress-strain relations during development of altered loads in chick embryo. *American Journal of Physiology-Heart and Circulatory Physiology*, *282*(6),

H2386–H2396. https://doi.org/10.1152/ajpheart.00879.2001

Yamazaki, Y., Sejima, H., Yuguchi, M., Namba, Y., & Isokawa, K. (2007). Late Deposition of Elastin to Vertical Microfibrillar Fibers in the Presumptive Dermis of the Chick Embryonic Tarsometatarsus. *The Anatomical Record: Advances in Integrative Anatomy and Evolutionary Biology*, *290*(10), 1300–1308. https://doi.org/10.1002/ar.20586